Effect of uneven magnetization on magnetic noise and vibrations in PMSM – application to EV HEV electric motor NVH

E. DEVILLERS, P. GNING, J. LE BESNERAIS

***Abstract* -- This paper studies the effect of uneven pole magnetization on acoustic noise and vibrations radiated by Permanent Magnet Synchronous Machines (PMSM) under Maxwell force excitations in open-circuit condition and on the full speed range.**

First, the effect of magnetic asymmetries is analyzed using analytic equations based on permeance / magnetomotive force. Then, electromagnetic, structural and acoustic calculations are performed using MANATEE software on a 48s8p Interior PMSM used in EV / HEV applications. To speed up calculations under asymmetrical conditions due to magnetization variations, Electromagnetic Vibration Synthesis algorithm is used. Simulation results show that uneven pole magnetization significantly affects airborne noise and vibrations, inducing low frequency noise and new resonances with structural modes which are not predicted by the GCD rule on pole/slot combination.

***Index Terms*—electrical machines, powertrain, e-NVH simulation, uneven magnetization**

I. INTRODUCTION

The design of electric powertrains for EV/HEV applications includes optimizing Noise, Vibrations and Harshness (NVH) performances, especially those due to the electromagnetic forces generated by the e-motor and referred as e-NVH. e-motors are designed to have high power density, which also means that their structure is subject to high magnetic stress. Such high power density can be achieved by choosing permanent magnets as rotor excitation which could lead to major issues in terms of e-NVH. Besides, the intrinsic variable speed property of powertrains imply additional e-NVH risks due to switching noise and the fact that resonance effect probability increases with speed range.

Furthermore, several e-NVH risks needs to be addressed at design stage. A detailed transfer path analysis of the powertrain can help to identify main e-NVH risks [1]:

- airborne noise due to vibrations of the outer structure which propagate to the air. Airborne noise then arises from the direct excitation of the outer structure, generally by radial forces applying at the interface between stator and airgap.
- structure borne noise from various origins, the main ones being excitations (such as Unbalance Magnetic Pull (UMP) or torque ripple) applying on the rotor and propagating to the outer structure through the bearings or directly exciting transmission gears.

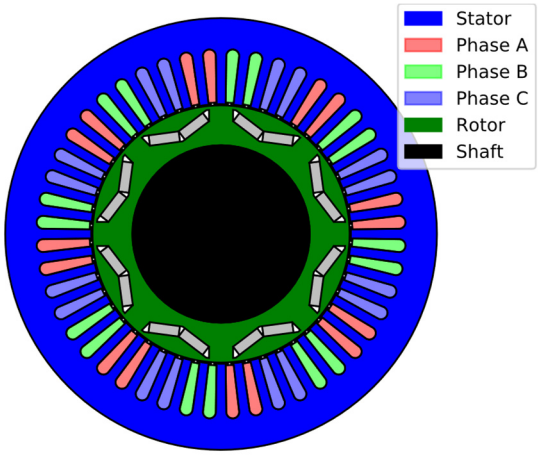

Fig. 1 IPMSM 48s8p topology from Toyota Prius 2004

Among e-motor topologies used in EV/HEV powertrains, the Interior Permanent Magnet Synchronous Machine with Zs=48 stator slots and 2p=8 poles (hereafter noted IPMSM 48s8p), as initially used in Toyota Prius 2004 powertrain, has become one of the main IPMSM design and especially because this particular topology demonstrates only a few e-NVH risks among those detailed earlier. In fact, the 3-phases integral distributed windings associated to the high pole number enables to lower the risk of exciting radial modes by considering the well-known GCD rule, with GCD(Zs,2p)=8 sufficiently high so that only pulsating forces may excite the structure and generate noise, especially within some specific speed ranges where those pulsating forces resonate with the breathing mode [2][3].

However, powertrains produced in large series generally present other e-NVH risks due to manufacturing tolerance and faults, including rotor eccentricity [4], stator bore ovality [5], uneven magnetization [6]. This article proposes to further study the impact of uneven pole magnetization on the e-NVH performances of the IPMSM 48s8p topology at open-circuit (no-load) condition. e-NVH simulations and post-processings are performed within MANATEE software [7]. Variable-speed acoustic results (spectrograms, order tracking, deflection shapes) are discussed and analyzed.

It is shown that uneven magnetization can lead to several e-NVH issues in the IPMSM 48s8p, such as inducing low frequency noise and new resonances with structural modes of high radiation efficiency. These resonances are not predicted by the GCD rule while they considerably increase the overall emitted noise.

E. Devillers, P. Gning and J. Le Besnerais are with EOMYS ENGINEERING, 121 rue de Chanzy, Lille-Hellemmes, France (website: www.eomys.com, e-mail: contact@eomys.com).

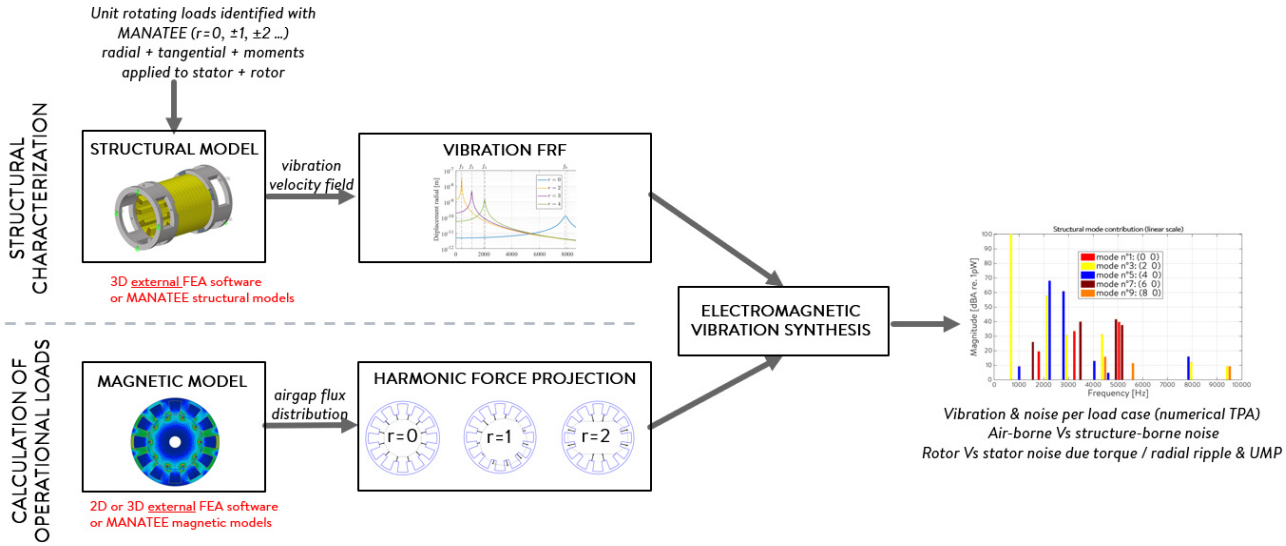

Fig. 2 Electromagnetic Vibration Synthesis (EVS) principle using MANATEE software [7]

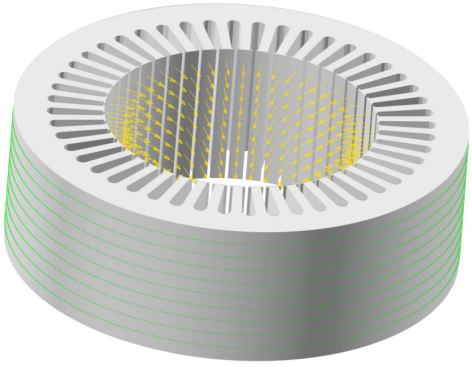

Fig. 3 3D FEA structural model of the stator with tooth tips loads in yellow and outer yoke response nodes in green

TABLE 1. ELASTIC PROPERTIES OF LAMINATION M400-50A

Young modulus [MPa]		Shear modulus [MPa]		Poisson ratio	
E_x	215	G_{xy}	82.7	ν_{xy}	0.3
E_y	215	G_{yz}	2	ν_{yz}	0.03
E_z	80	G_{zx}	2	ν_{zx}	0.03

II. SIMULATION WORKFLOW

A. *Electromagnetic model*

1) *Theoretical force analysis*

Electromagnetic forces considered in this study are Maxwell forces applying on stator structure and concentrated at iron/air interface. Maxwell force distribution, or Maxwell stress, is decomposed in elementary travelling harmonic waves of electrical frequency f and wavenumber r noted $\{f,r\}$. The frequency f is the frequency of force, vibration and acoustic noise. The wavenumber is the spatial frequency (i.e. number of maximums or minimums) of the stress wave and its sign indicates the rotation direction of the force wave.

Stress waves with wavenumber r=0 are pulsating waves, whose frequency is proportional to LCM(Zs,2p)f_s/p=12f_s (noted H48 in terms of mechanical order). Stress waves with wavenumber different of 0 are rotating waves. The lowest wavenumber is given by GCD(Zs,2p)=8. Therefore, all airgap stress wavenumbers are either 0 or proportional to 8. All pulsating stress waves are surrounded by two rotating sidebands of frequency ±2f_s (±H8) and wavenumber ∓8.

Uneven magnetization completely breaks the periodicity given by the number of pole pairs: all magnetic poles are different. Therefore, all mechanical orders and wavenumbers are present in Maxwell stress harmonic content.

2) *Flux density computation*

The radial and tangential airgap flux densities in open-circuit condition are computed using MANATEE fast hybrid model coupling Subdomain Model (SDM) and Finite Element Analysis (FEA) [8]. Uneven magnetization is introduced by a adding a randomization of ±5% on the remanent flux density of each pole.

3) *Magnetic force computation*

Radial and tangential magnetic stress on the stator structure are obtained by computing the Maxwell stress tensor at the middle of the air gap, such as:

$$\sigma_{rad}(t,\theta) = \frac{B_{rad}^2(t,\theta) - B_{tan}^2(t,\theta)}{2\mu_0} \ [N.m^{-2}] \qquad (1)$$

$$\sigma_{tan}(t,\theta) = \frac{B_{rad}(t,\theta)B_{tan}(t,\theta)}{\mu_0} \ [N.m^{-2}] \qquad (2)$$

Radial and tangential Maxwell stress distributions are decomposed in stress waves by means of 2D Fourier Transform (FFT).

B. *e-NVH model*

1) *Electromagnetic Vibration Synthesis (EVS)*

Vibrations of the housing envelope are calculated using Electromagnetic Vibration Synthesis process (EVS) [9]. EVS principle is illustrated in Fig. 2. It consists in computing separately electromagnetic operational loads and structural response under unit-magnitude loads (Frequency Response Functions, FRF) and then making the synthesis to get operational vibrations.

2) *Mechanical model*

FRF are obtained from a 3D FEA model using MANATEE coupling with Hypermesh/Optistruct [10]. To compute FRF, unit-magnitude force waves are applied on stator tooth tips and displacement are taken for all nodes belonging to stator yoke outer surface, as illustrated in Fig. 3. The stator yoke is clamped at bottom end. Stator material properties are given in

Table 1. Reduced damping is set to 2%. Stator windings are not included in the model.

To perform EVS with uneven magnetization assumption, FRF are computed for any wavenumbers between -8 and 8 and in both radial and tangential directions. Wavenumbers for which absolute value is larger than 8 are neglected in the following. They should not radiate airborne noise due to high yoke stiffness.

3) *Acoustics model*

A-weighted Sound Power Level (noted A-SWL) is calculated using Equivalent Radiated Power (ERP). ERP calculation method is known to overestimate "low frequency" acoustic noise level compared to finite element acoustic calculations. Vibration levels are indeed radiated with smaller efficiency below cut-off frequency of the body.

III. Simulation Results

A. *Open-circuit airgap flux density and space FFT*

1) *Even pole magnetization*

Fig. 4 shows airgap radial flux density with even magnetization in function of space (over one pole pair) and its harmonic content. All space harmonics are multiple of periodicity factor which is 4.

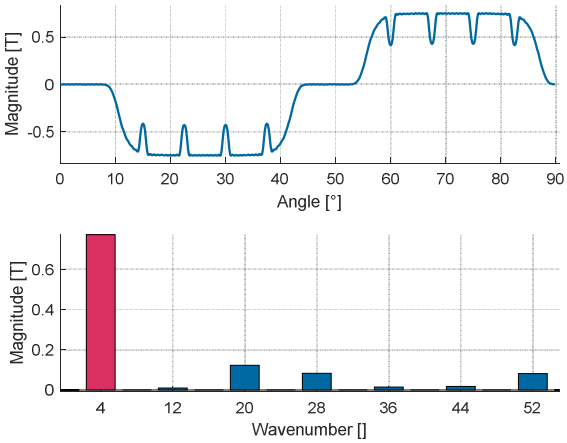

Fig. 4 Radial airgap flux density and FFT, even magnetization

2) *Uneven pole magnetization*

Fig. 5 shows airgap radial flux density with uneven magnetization in function of space and its harmonic content. Compared to the even magnetization case, uneven magnetization introduced space harmonics for all wavenumbers, especially sub-harmonics for r=1,2,3.

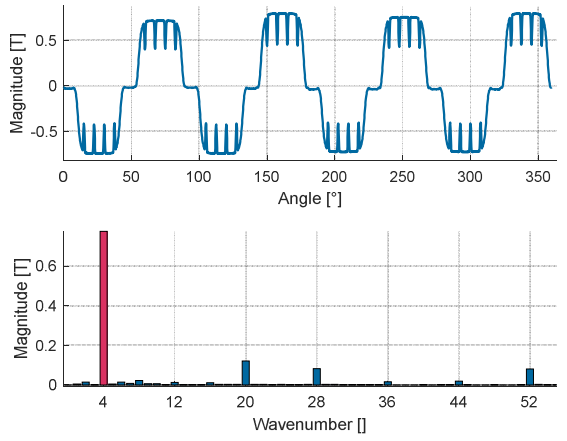

Fig. 5 Radial airgap flux density and FFT, uneven magnetization

B. *Open-circuit magnetic forces*

1) *Even pole magnetization*

Time and space harmonic content of radial stress is illustrated in Fig. 6. As described in theoretical part II. A. 1) , all wavenumbers are multiple of 8. Then, pulsating harmonics have mechanical orders multiple of 48 and are surrounded by two rotating forces of mechanical order ±H8 and wavenumber r=∓8. Same harmonic content is found for tangential stress.

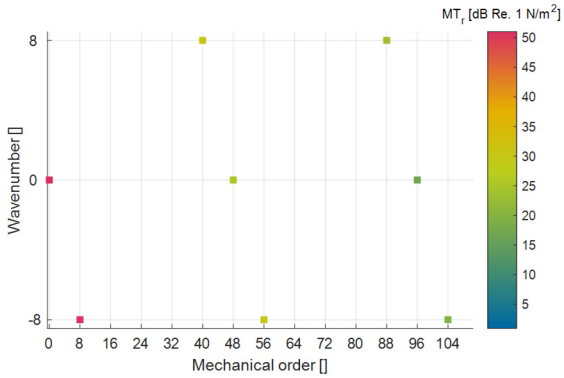

Fig. 6 FFT 2D of radial airgap stress, even magnetization

2) *Uneven pole magnetization*

Uneven magnetization introduced new stress harmonics as sidebands of existing harmonics in even magnetization condition (cf. Fig. 7). Therefore, all mechanical orders and wavenumbers exist in the 2D FFT of radial magnetic stress. Same harmonic content is found for tangential stress.

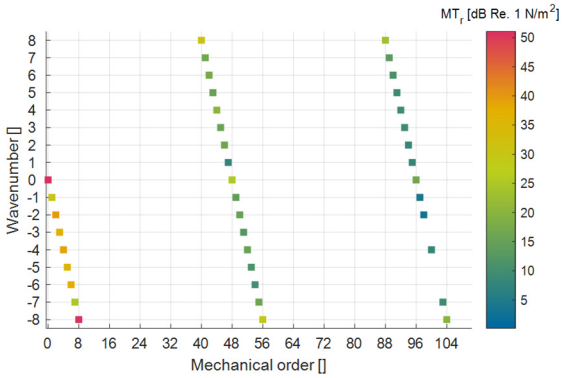

Fig. 7 FFT 2D of radial airgap stress, uneven magnetization

C. *Structural response*

1) *Main structural modes*

Main stator structural modes are obtained from numerical modal analysis and presented in Table 2. The main mode of interest is the breathing mode around 5450 Hz (cf. Fig. 8) which is likely to be excited by radial pulsating forces. Other radial modes (m={1,2,3,4}, n=0) can be excited in uneven magnetization condition since all wavenumbers exist in magnetic radial stress harmonic content. Besides, both tooth bending modes at 4513 and 4519 Hz are likely to be excited by tangential stress harmonics of wavenumber r=±8

TABLE 2 ORDERS AND NATURAL FREQUENCIES OF STRUCTURAL MODES

Mode identification (m,n) (m: circumferential order; n: longitudinal order)	Natural frequency (Hz)
Yoke "breathing" mode (0,0)	5450
Yoke 'bending modes (1,0)	963 & 970
Yoke "ovalization" modes (2,0)	995 & 1000
Radial modes (3,0)	1732 & 1737
Radial modes (4,0)	2698 & 2703
Tooth bending modes (8,0)	4513 & 4519

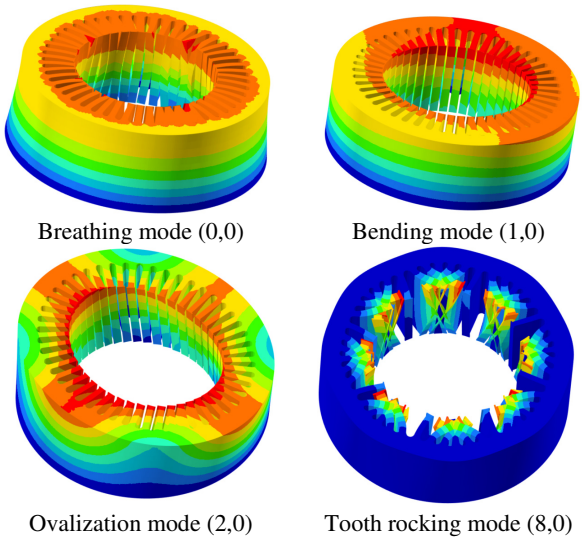

Fig. 8 Modal shapes of several structural modes

2) *Displacement FRF, r=0,2,8*

RMS value of displacement FRF under radial (respectively tangential) unit-magnitude force waves of wavenumber r=0,2,8 are illustrated in Fig. 9 (respectively Fig. 10). RMS displacement value is obtained by averaging the squared displacement value for each node of the outer yoke surface (cf. Fig. 3).

In even magnetization case, vibrations are only due to FRF associated to wavenumbers r=-8,0,8. Therefore, main resonance peaks are due to radial pulsating (r=0) force waves resonating with breathing mode around 5450 Hz and tangential rotating forces (r=±8) resonating with tooth bending mode around 4500 Hz.

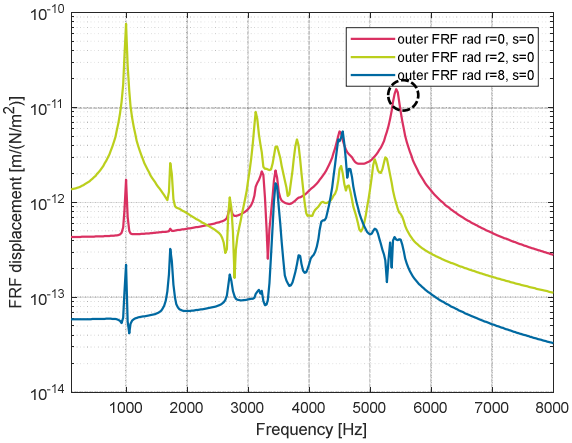

Fig. 9 FRF for radial unit-magnitude force waves, r=0,2,8

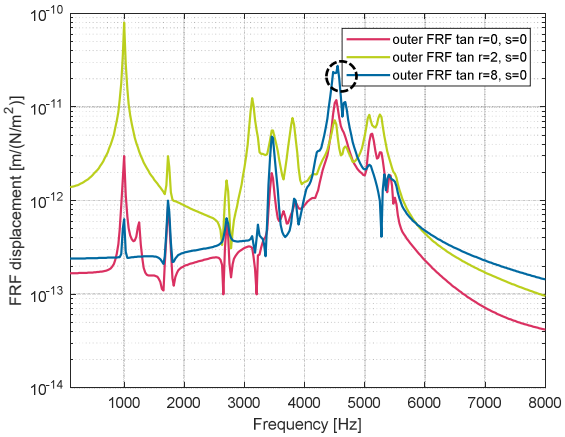

Fig. 10 FRF for tangential unit-magnitude force waves, r=0,2,8

Tooth bending mode contribution is overestimated in the mechanical response since stator winding is not modelled.

D. *e-NVH results: spectrograms, order tracking and ODS*

1) *Even pole magnetization*

Variable-speed A-weighted Sound Power Level (A-SWL) resulting for EVS and ERP in even pole magnetization is illustrated in terms of spectrogram (Fig. 11), order tracking analysis (Fig. 12), force wavenumber contribution (Fig. 13).

Spectrogram and order tracking analysis enable to state on force waves and structural modes interaction and to troubleshoot resonance origins. The main resonance peak (straw yellow mark) is due to the interaction of main pulsating force at H48 with breathing mode around 5450 Hz and 6800 rpm. The second resonance peak (light purple mark) comes from both stator tooth bending modes (m=8, n=0) excited by tangential rotating force waves around 4520 Hz and at 4844 rpm. ODS at those two resonances are illustrated in Fig. 14.

In Fig. 13, force wavenumber contribution mixing radial and tangential excitations including positive and negative wavenumbers is expressed in percentage of overall A-SWL. Tooth bending mode contribution increases up to 20% of the acoustic sound power at main resonance peak (5450 Hz and 6800 rpm). However, this contribution is overestimated in the simulation since stator winding is not modelled and would considerably increase stator stiffness regarding tooth bending motion.

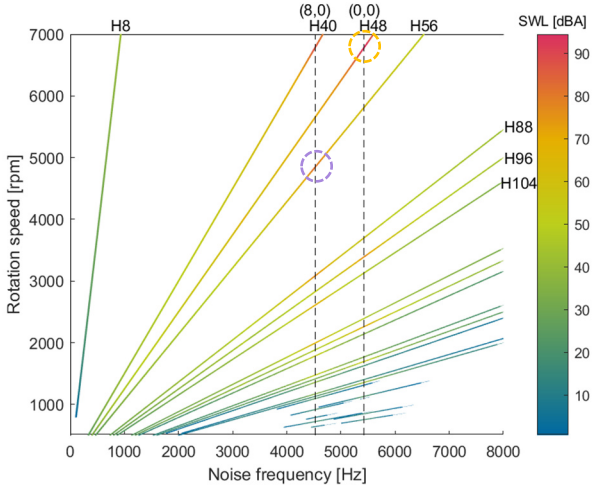

Fig. 11 A-SWL spectrogram, even magnetization

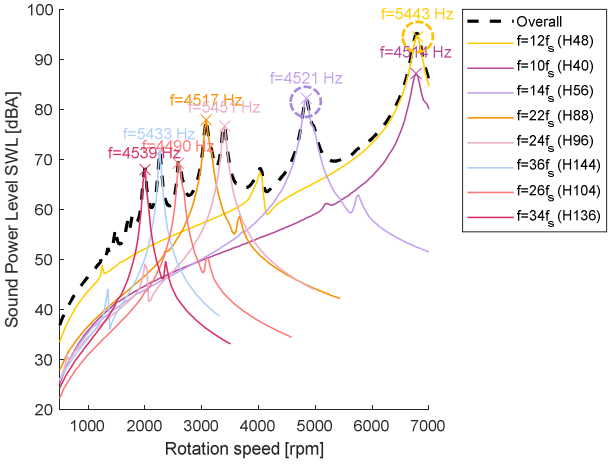

Fig. 12 Order tracking analysis, even magnetization

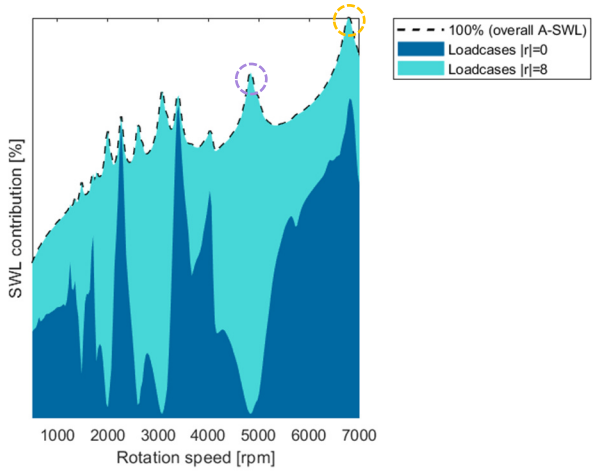

Fig. 13 Wavenumber contribution to A-SWL, even magnetization

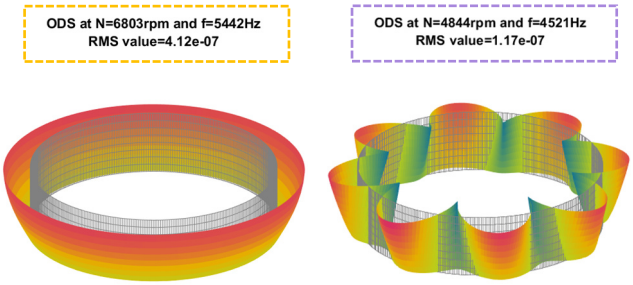

Fig. 14 ODS at the two main resonances, even magnetization

2) *Uneven pole magnetization*

Same variable-speed A-SWL post-processings are performed for the uneven pole magnetization case. The spectrogram in Fig. 15 shows much more orders as expected from the magnetic stress spectrum illustrated in Fig. 7. The two main resonances highlighted in the even magnetization case are still present in uneven magnetization case, even if colors have changed to match with order tracking for uneven magnetization in Fig. 16. In fact, main e-NVH risk remains the excitation of breathing mode by radial pulsating forces.

Besides, sideband excitations due to uneven magnetization lead to new resonances with stator radial modes hence to a large increase of A-SWL, in particular at low-speed and low-frequency. A first resonance peak can be observed around 1000 Hz and 1320 rpm due to the interaction of (H46, r=-2) stress wave with ovalization mode, as confirmed by stator yoke ODS in Fig. 18. A second resonance peak occurs around 1720 Hz and 3000 rpm due to the interaction of (H45, r=-3) stress wave with radial mode (m=3, n=0), cf. ODS in Fig. 18. (H44, r=-4) stress wave also resonates with radial mode (m=4, n=0) around 2690 Hz and 3700 rpm.

Hence, all radial modes are successively excited due to magnetic force waves arising from uneven magnetization which considerably increase the overall A-SWL. This is again visible on force wavenumber contribution (cf. Fig. 17), which also confirms that high wavenumber force waves (e.g. $|r|$=5,6,7,8 etc.) have a negligible impact on emitted noise.

IV. Conclusion

The effect of uneven pole magnetization has been studied based on e-NVH simulation results for the IPMSM 48s8p study case at variable-speed open-circuit condition. The main noise issue is already present for even magnetization and comes from the excitation of the outer structure breathing mode by radial pulsating forces. Tangential rotating forces

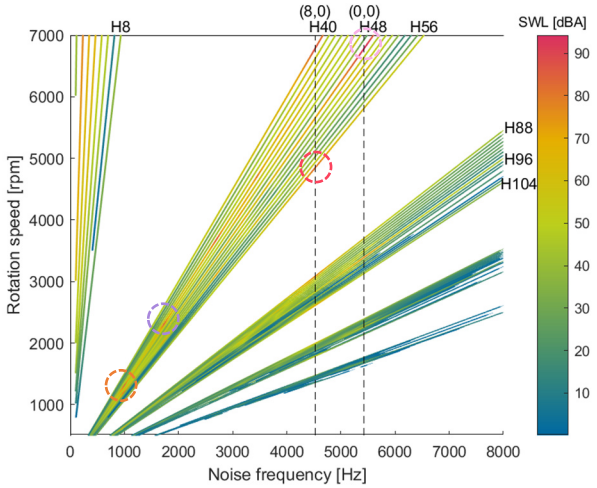

Fig. 15 A-SWL spectrogram, uneven magnetization

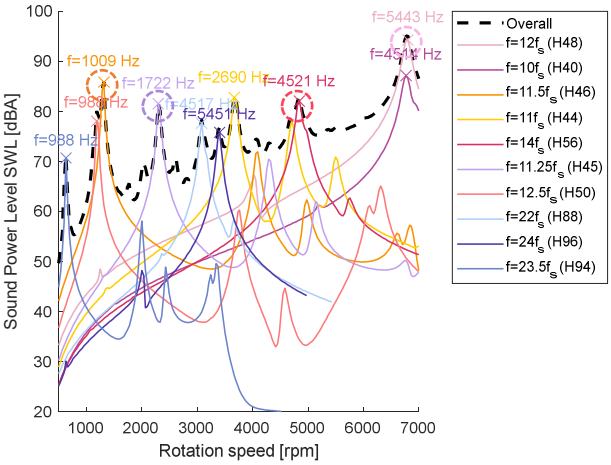

Fig. 16 Order tracking analysis, uneven magnetization

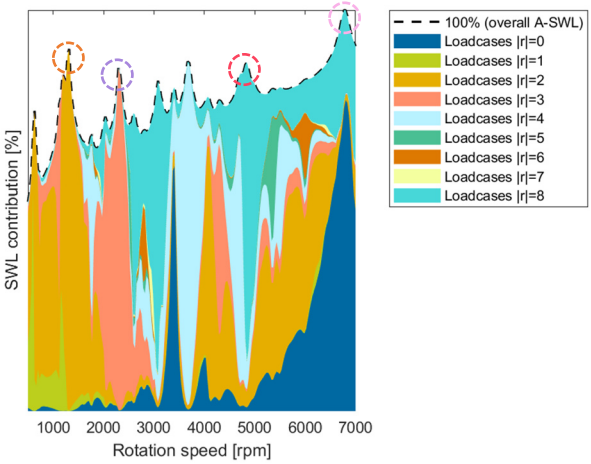

Fig. 17 Wavenumber contribution to A-SWL, uneven magnetization

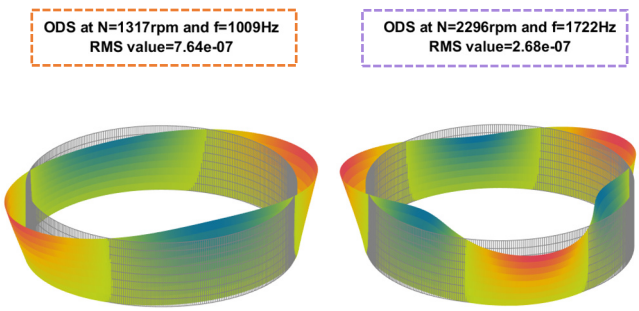

Fig. 18 ODS at two new resonances induced by uneven magnetization

can also induce outer surface vibrations due to tooth bending modes in case of low stator stiffness.

It has been shown that uneven magnetization is a major e-NVH risk which may considerably increase overall noise level on the whole speed range by inducing low frequency noise and new resonances with structural modes of high radiation efficiency. These resonances are not predicted by the GCD rule based on slot/pole combination which becomes a poor e-NVH criterion in fault condition.

To go further, uneven magnetization also generates unbalanced forces (UMP) on both rotor and stator structures, which may also have an impact on structure borne noise. Besides, uneven magnetization can also occur in the axial direction, particularly in case of multi-layer skewed rotor topologies which are originally designed to reduce torque and force ripple. Uneven magnetization in axial direction generates axial forces which can be source of structure borne noise. It also leads to a longitudinal variation of radial and tangential force distributions which can excite other modes of the outer structure, increasing air borne noise.

V. References

[1] M. Boesing, "Noise and Vibration Synthesis based on Force Response Superposition," Fakultät für Elektrotechnik und Informationstechnik der Rheinisch-Westfälischen Technischen Hochschule Aachen, 2013.

[2] A. Hofmann, F. Qi, T. Lange, and R. W. De Doncker, "The breathing mode-shape 0: Is it the main acoustic issue in the PMSMs of today's electric vehicles?," in *2014 17th International Conference on Electrical Machines and Systems (ICEMS)*, 2014, pp. 3067–3073.

[3] Z. Yang, M. Krishnamurthy, and I. P. Brown, "Electromagnetic and vibrational characteristic of IPM over full torque-speed range," in *2013 International Electric Machines and Drives Conference*, 2013, pp. 295–302.

[4] A. Rezig, M. R. Mekideche, and A. Djerdir, "Effect of Rotor Eccentricity Faults on Noise Generation in Permanent Magnet Synchronous Motors," *Prog. Electromagn. Res. C*, vol. 15, no. July, pp. 117–132, 2010.

[5] J. Le Besnerais, "Effect of lamination asymmetries on magnetic vibrations and acoustic noise in synchronous machines," in *2015 18th International Conference on Electrical Machines and Systems (ICEMS)*, 2015, vol. 48, no. may, pp. 1729–1733.

[6] D. Torregrossa, A. Khoobroo, and B. Fahimi, "Prediction of acoustic noise and torque pulsation in PM synchronous machines with static eccentricity and partial demagnetization using field reconstruction method," *IEEE Trans. Ind. Electron.*, vol. 59, no. 2, pp. 934–944, 2012.

[7] Eomys Engineering, "MANATEE v1.09.01," 2020. [Online]. Available: http://www.manatee-software.com.

[8] E. Devillers, M. Hecquet, and J. Le Besnerais, "A new hybrid method for the fast computation of airgap flux and magnetic forces in IPMSM," in *2017 Twelfth International Conference on Ecological Vehicles and Renewable Energies (EVER)*, 2017, pp. 1–8.

[9] M. van der Giet, "Analysis of electromagnetic acoustic noise excitations: A contribution to low-noise design and to the auralization of electrical machines," Rheinisch-Westfalische Technische Hochschule Aachen, 2011.

[10] Altair, "OptiStruct," *www.altairhyperworks.com/product/OptiStruct*, 2018.

VI. Biographies

E. Devillers has done an industrial PhD thesis at EOMYS ENGINEERING (Lille, France) and L2EP laboratory of the Ecole Centrale de Lille, North of France and graduated in 2018. He is now researcher and software developer at EOMYS. His research interests are the modeling of noise and vibrations in electrical machines due to magnetic forces for reduction purposes.

P. Gning currently works for EOMYS ENGINEERING as an R&D engineer on e-NVH of electrical machines. Following a M. Sc. specialized in Applied Mechanics (UTC, France) in 2014, he made an industrial PhD thesis from 2015 to 2018 at Roberval (UTC, France) laboratory with RTE, focusing on noise and vibration root cause analysis and reduction techniques of industrial reactors. His research interests are the modeling and testing of noise and vibrations in electrical devices.

J. Le Besnerais currently works in EOMYS ENGINEERING as an R&D engineer on the analysis and reduction of acoustic noise and vibrations in electrical systems.

Following a M.Sc. specialized in Applied Mathematics (Ecole Centrale Paris, France) in 2005, he made an industrial PhD thesis in Electrical Engineering at the L2EP laboratory of the Ecole Centrale de Lille, North of France, on the reduction of electromagnetic noise and vibrations in traction induction machines with ALSTOM Transport. He worked from 2008 to 2013 as an engineer in the railway and wind industries (Alstom, Siemens Wind Power, Nenuphar Wind) on some multiphysic design and optimization tasks at system level (heat transfer, acoustic noise and vibrations, electromagnetics, structural mechanics and aerodynamics). In 2013, he founded EOMYS ENGINEERING, a company providing applied research and development services including modeling and simulation, scientific software development and experimental measurements.